Time dependent *CP*-even and *CP*-odd signatures of scalar ultralight dark matter in neutrino oscillations

Marta Losada,[1,*] Yosef Nir,[2,†] Gilad Perez,[2,‡] Inbar Savoray,[2,§] and Yogev Shpilman[2,‖]
[1]*New York University Abu Dhabi, PO Box 129188, Saadiyat Island, Abu Dhabi, United Arab Emirates*
[2]*Department of Particle Physics and Astrophysics, Weizmann Institute of Science, Rehovot 7610001, Israel*

(Received 2 April 2023; accepted 8 August 2023; published 6 September 2023)

Scalar ultralight dark matter (ULDM) interacting with neutrinos can induce, under certain conditions, time dependent modifications to neutrino oscillation probabilities. The limit in which the ULDM perturbation can be treated as constant throughout the neutrino propagation time has been addressed by several previous works. We complement these by systematically analyzing the opposite limit—accounting for the temporal variations of the ULDM field by solving time dependent Schrödinger equations. In particular, we study a novel two-generations-like *CP* violating (CPV) signature unique to rapidly oscillating ULDM. We derive the leading order, time dependent corrections to the oscillation probabilities, for both *CP* conserving and CPV couplings, and explain how they can be measured in current and future experiments.

DOI: 10.1103/PhysRevD.108.055004

I. INTRODUCTION

Scalar ultralight dark matter (ULDM) with mass $m_\phi \lesssim$ eV may leave signatures in neutrino oscillation experiments that cannot be interpreted within the Standard Model (SM) supplemented by neutrino masses and lepton mixing. The scalar can be treated as a classical bosonic field that oscillates with time,

$$\phi = \phi_0 \sin(m_\phi (t - t_0)), \tag{1}$$

with an arbitrary initial time t_0 and amplitude

$$\phi_0 = \frac{\sqrt{2\rho_\phi^\oplus}}{m_\phi} \sim 2\ \text{GeV}\left(\frac{10^{-12}\ \text{eV}}{m_\phi}\right), \tag{2}$$

where $\rho_\phi^\oplus$ is the local ULDM density. Consider the effective mass and ϕ-Yukawa terms for the neutrinos, arising from dimension-five and dimension-six terms in the Lagrangian, respectively. In the basis in which the ULDM-independent mass matrix is diagonal, they read

$$\mathcal{L}_{m_\nu} = m_i \nu_i^T \nu_i + \hat{y}_{ij} \phi \nu_i^T \nu_j + \text{H.c.} \tag{3}$$

Treating ϕ as a classical field, it modifies the neutrino mass matrix as

$$(\hat{m}_\nu)_{ij} = m_i \delta_{ij} + \hat{y}_{ij} \phi, \tag{4}$$

thus inducing a time dependent component to the neutrino propagation Hamiltonian.

Some of the implications of the ULDM contribution to the neutrino mass matrix have been studied in previous works [1–12]. Most previous analyses focused on ULDM candidates with typical oscillation times, $\tau_\phi \equiv 2\pi/m_\phi$, much larger than the neutrino propagation time, τ_d, but smaller than the total run-time of the experiment, τ_e [1,4–6]. In this limit, the effective neutrino masses and mixing do not change during the propagation from the source to the detector, but do change between neutrino events over the duration of the experiment. Depending on the value of m_ϕ, the experiment time resolution τ_r, and the way one analyzes the data, the ULDM effect can be either time-resolved or time-averaged. In the former case, the temporal modulation could be directly observed in some spectral analysis of the data [5,6]. In the latter case, the oscillatory contributions are averaged out, and one must use indirect methods for recovering evidence of the time dependence, e.g., via the distortion of the dynamical range of the neutrino oscillation parameters or of relations between oscillation amplitudes at different L/E frequencies [1,5–7] (L is the source to detector distance and E is the neutrino energy).

However, the experimental signatures of heavier ULDM, with $\tau_\phi \lesssim \tau_d$, require a dedicated analysis. In the limit of rapid oscillations, one must solve time dependent equations

*marta.losada@nyu.edu
†yosef.nir@weizmann.ac.il
‡gilad.perez@weizmann.ac.il
§inbar.savoray@weizmann.ac.il
‖yogev.shpilman@weizmann.ac.il

of motion to correctly account for the ULDM effects on neutrino oscillation probabilities, and the picture of slowly varying oscillation parameters is no longer valid [5,13]. In addition, thus far, the majority of previous works discussing ULDM-modified neutrino oscillations have only considered *CP* conserving (CPC) couplings. *CP* violating (CPV) effects in neutrino oscillations induced by ULDM-neutrino interactions have been analyzed by authors of this manuscript in Ref. [6], for the case of slow oscillations. Furthermore, past works have either studied specific flavor structures for the ULDM couplings [2,6,7] or studied the "model-agnostic" temporal modulations of the mixing angles, mass differences, and the CPV phase of the Pontecorvo–Maki–Nakagawa–Sakata (PMNS) matrix [1,5,6]. To the best of our knowledge, the relations between the ULDM couplings and these variations of oscillation parameters have not been explicitly discussed and could be nontrivial (both mathematically and phenomenologically). Therefore, translating the conclusions of the existing analyses to generic ULDM models could be challenging.

In this work, we fill in those gaps and provide a more complete description of the phenomenology of ULDM-neutrino couplings. We are interested in mapping those couplings onto their signatures in neutrino oscillation experiments, for a wide range of ULDM masses, covering both the slow oscillations and the rapid oscillations limits. We present a generic prescription for estimating the first-order, time dependent modifications to neutrino oscillations from ULDM couplings to neutrinos, and the resulting bounds on them from current and future experiments. While we study both CPC and CPV phenomena, we give special attention to the implications of the CPV ULDM couplings. In particular, we describe new CPV effects generated by them that can be observable even in two-generation neutrino systems and cannot be addressed by analyses assuming a constant neutrino Hamiltonian through propagation.

The paper is organized as follows. In Sec. II, we describe the new CPV effect in the two neutrino generations picture—which we refer to as the "2-ν CPV." In Sec. III, we derive the full analytical expressions for the leading order modifications to neutrino oscillation probabilities induced by the ULDM, for both CPC and CPV phenomena. In Sec. IV, we describe the method for detecting such time dependent modifications in neutrino oscillations data. In Sec. V, we show the current bounds, and the future-projected sensitivities, for the ULDM parameter space. We conclude in Sec. VI.

II. 2-ν *CP* VIOLATION

We are interested in the possibility of observing CPV in neutrino oscillations induced by the time dependent vacuum expectation value (VEV) of ϕ. In the usual two-generation picture, one can show that by field redefinitions, the mass matrix $\hat{m}_\nu$ can always be brought to a form in which it has no physical phases affecting neutrino oscillations (see, e.g., [14,15]), and thus CPV cannot be observed in these processes. This can be seen by the following simple argument. In the two-neutrino picture, the equation of motion (EOM) is given by[1]

$$i\partial_t \begin{pmatrix} \nu_\alpha \\ \nu_\beta \end{pmatrix} = \mathcal{H}(t) \begin{pmatrix} \nu_\alpha \\ \nu_\beta \end{pmatrix} = \begin{pmatrix} \mathcal{H}_{11} & \mathcal{H}_{12} e^{i\varphi} \\ \mathcal{H}_{12} e^{-i\varphi} & \mathcal{H}_{22} \end{pmatrix} \begin{pmatrix} \nu_\alpha \\ \nu_\beta \end{pmatrix}. \quad (5)$$

Since the Hamiltonian $\mathcal{H}$ is Hermitian, $\mathcal{H}_{ij}$ and φ above must be real. Let $\nu_i(t)$ be the time-evolved state, according to Eq. (5), which was ν_i at $t = 0$. If $\nu_{\alpha,\beta}$ are interaction eigenstates, then the initial conditions at $t = 0$ are zero for one of them, and one for the other, and the probability for detecting the states $\nu_{\alpha,\beta}$ at some later time t is given by solving the EOM and calculating

$$P_{\nu_i \to \nu_f} = |\langle \nu_f | \nu_i(t) \rangle|^2. \quad (6)$$

While $\mathcal{H}$ carries a CPV Majorana phase φ, it can be absorbed in the redefinition of the field $\nu'_\beta = e^{i\varphi}\nu_\beta$, which makes the EOM real

$$i\partial_t \begin{pmatrix} \nu_\alpha \\ \nu'_\beta \end{pmatrix} = \mathcal{H}'(t) \begin{pmatrix} \nu_\alpha \\ \nu'_\beta \end{pmatrix} = \begin{pmatrix} \mathcal{H}_{11} & \mathcal{H}_{12} \\ \mathcal{H}_{12} & \mathcal{H}_{22} \end{pmatrix} \begin{pmatrix} \nu_\alpha \\ \nu'_\beta \end{pmatrix}. \quad (7)$$

In the context of neutrino oscillations, this field redefinition has no physical significance, since ν'_β is still a flavor eigenstate, and the oscillation probabilities for any ν' and ν states that are related by arbitrary phases $\nu'_{\alpha,\beta} = e^{i\varphi_{\alpha,\beta}}\nu_{\alpha,\beta}$ are the same, since

$$P_{\nu'_i \to \nu'_f} = |\langle \nu'_f | \nu'_i(t) \rangle|^2 = |\langle \nu_f | e^{i(\varphi_i - \varphi_f)} | \nu_i(t) \rangle|^2 = P_{\nu_i \to \nu_f}. \quad (8)$$

For antineutrinos, which are the *CP* conjugates of ν, i.e., $\bar{\nu} = i\sigma_2 \nu^*$, the EOM is given by

$$i\partial_t \begin{pmatrix} \bar{\nu}_\alpha \\ \bar{\nu}_\beta \end{pmatrix} = \mathcal{H}^*(t) \begin{pmatrix} \bar{\nu}_\alpha \\ \bar{\nu}_\beta \end{pmatrix}, \quad (9)$$

and thus we may again redefine our fields as $\overline{\nu'}_\beta = e^{-i\varphi}\bar{\nu}_\beta$ and obtain

$$i\partial_t \begin{pmatrix} \bar{\nu}_\alpha \\ \overline{\nu'}_\beta \end{pmatrix} = \mathcal{H}'(t) \begin{pmatrix} \bar{\nu}_\alpha \\ \overline{\nu'}_\beta \end{pmatrix}. \quad (10)$$

We then learn that, since $\mathcal{H}'$ does not depend on φ, antineutrinos propagate like neutrinos.

[1]A similar Hamiltonian was studied in [16,17], exploring the possibility of magnetic interactions of neutrinos.

In the presence of the oscillating ULDM background, $\phi(t)$, the CPV phase, φ, could become time dependent. Then, the field redefinition $\nu'_\beta = e^{i\varphi(t)}\nu_\beta$ yields

$$i\partial_t \begin{pmatrix} \nu_\alpha \\ \nu'_\beta \end{pmatrix} = \begin{pmatrix} \mathcal{H}_{11} & \mathcal{H}_{12} \\ \mathcal{H}_{12} & \mathcal{H}_{22} - \dot{\varphi} \end{pmatrix} \begin{pmatrix} \nu_\alpha \\ \nu'_\beta \end{pmatrix}, \tag{11}$$

for neutrinos, and

$$i\partial_t \begin{pmatrix} \bar{\nu}_\alpha \\ \overline{\nu'}_\beta \end{pmatrix} = \begin{pmatrix} \mathcal{H}_{11} & \mathcal{H}_{12} \\ \mathcal{H}_{12} & \mathcal{H}_{22} + \dot{\varphi} \end{pmatrix} \begin{pmatrix} \bar{\nu}_\alpha \\ \overline{\nu'}_\beta \end{pmatrix}, \tag{12}$$

for antineutrinos. Note that the oscillation probabilities for ν and ν' are still identical, since Eq. (8) still holds even when promoting φ to be time dependent. Thus, neutrinos and antineutrinos would evolve differently in time, as a result of the time dependent Majorana phase.

While the instantaneous phase of the fields is not physically observable, its derivative—which can be thought of as an instantaneous frequency—shifts the energy of the system and is thus observable. Indeed, the Hamiltonians in Eqs. (11) and (12) are very similar to those resulting from charged current matter effects, identifying $-\dot{\varphi}$ with the matter potential V_C [18]. Note that in our case $-\dot{\varphi}$ is a periodic function of time, which will ultimately result in a time periodic *CP* asymmetry.

For concreteness, let us explicitly examine this effect in a two-generation system. Consider the following Yukawa matrix $\hat{y}$ describing the ULDM coupling to the unperturbed mass eigenstates in two generations:

$$\hat{y} = iy_I \begin{pmatrix} 0 & 1 \\ 1 & 0 \end{pmatrix}, \tag{13}$$

with real y_I. Given the Yukawa interaction in Eq. (3) is Majorana-like, the most general form of $\hat{y}$ is $\hat{y} = a_\mu \sigma_\mu$, with $\mu = 0,\ 1,\ 3$, $\sigma_0 = \mathbf{1}_2$, $\sigma_{1,3}$ are the corresponding symmetric Pauli matrices, and the a_μ's are complex numbers. Note that within the two-generation framework, at any given time the unperturbed instantaneous PMNS matrix can be brought to be real, and so it is straightforward to show that the form of $\hat{y}$ written above uniquely leads to two-generation CPV. In the interaction basis, in the ultrarelativistic limit, the Hamiltonian can be written as

$$\begin{aligned} \mathcal{H} = \frac{1}{2E}\hat{m}_\nu^\dagger \hat{m}_\nu &\sim \frac{\Delta m^2}{4E}\begin{pmatrix} -\cos 2\theta & \sin 2\theta \\ \sin 2\theta & \cos 2\theta \end{pmatrix} \\ &+ \frac{\phi_0}{2E}\begin{pmatrix} 0 & -iy_I \Delta m \\ iy_I \Delta m & 0 \end{pmatrix} \sin(m_\phi (t - t_0)) \\ &+ \mathcal{O}\left(\frac{y_I^2 \phi_0^2}{E}\right), \end{aligned} \tag{14}$$

where θ is the mixing angle between the interaction eigenstates in the unperturbed mass eigenstates, $\Delta m = m_2 - m_1$, $\Delta m^2 = m_2^2 - m_1^2$, and a part of $\mathcal{H}$ proportional to the unit matrix was omitted as it does not contribute to neutrino oscillations. To leading order in the ULDM perturbation, we identify

$$\dot{\varphi} \approx -\frac{2m_\phi \phi_0 y_I}{(m_1 + m_2)\sin 2\theta}\cos(m_\phi (t - t_0)). \tag{15}$$

Following the prescription presented in the next section, the leading order difference between the survival probability of neutrinos $P_{\alpha\alpha}$ and the survival probability of antineutrinos $P_{\bar{\alpha}\bar{\alpha}}$ is given by

$$\begin{aligned} \Delta P^{(1)}_{\alpha\alpha} = &\frac{2\phi_0 \sin 4\theta y_I (m_1 - m_2)}{E\left(\left(\frac{\Delta m^2}{2E}\right)^2 - m_\phi^2\right)} \\ &\times \left[\cos\left(m_\phi\left((t - L - t_0) + \frac{L}{2}\right)\right)\right. \\ &\times \left(\frac{\Delta m^2}{4E}\sin\frac{\Delta m^2 L}{2E}\sin\frac{m_\phi L}{2}\right. \\ &\left.\left. - m_\phi \sin^2\frac{\Delta m^2 L}{4E}\cos\frac{m_\phi L}{2}\right)\right], \end{aligned} \tag{16}$$

where L is the distance that the neutrinos traveled between production and detection. In the following sections, we discuss the implications of this "2-ν CPV" effect, and how it can be searched for in neutrino oscillation experiments.

III. ANALYTIC APPROXIMATION FOR SMALL PERTURBATIONS

A. Generic prescription

The neutrino Schrödinger EOMs can be written as

$$\begin{aligned} i\partial_t \nu(t) &= \frac{1}{2E}(\hat{m}^\dagger \hat{m})\nu(t) \\ &= \frac{1}{2E}(m^\dagger m + (m^\dagger y + y^\dagger m)\phi(t) + y^\dagger y \phi^2(t))\nu(t). \end{aligned} \tag{17}$$

The solutions of systems with time dependent Hamiltonians $\mathcal{H}(t) = \mathcal{H}_0 + V(t)$ can be found using the Dyson series. A neutrino state at any final time point t_f is evolved from an initial neutrino state at time t_i as $|\nu(t_f)\rangle = \mathcal{U}(t_f, t_i)|\nu(t_i)\rangle$ with

$$\mathcal{U}(t_f,t_i)=\sum_{n=0}^{\infty}\mathcal{U}^{(n)}(t_f,t_i)$$
$$\equiv e^{-i\mathcal{H}_0(t_f-t_i)}+\sum_{n=1}^{\infty}(-i)^n\int_{t_f\geq t_1\ldots\geq t_n\geq t_i}dt_1\ldots dt_n e^{-i\mathcal{H}_0(t_f-t_1)}V(t_1)e^{-i\mathcal{H}_0(t_1-t_2)}\ldots V(t_n)e^{-i\mathcal{H}_0(t_n-t_i)}. \quad (18)$$

The probability for a neutrino produced in a state ν_α at time t_i to be measured as neutrino state ν_β at a later time t_f is

$$P_{\alpha\beta}(t_f)=|\langle\nu_\beta|\mathcal{U}(t_f,t_i)|\nu_\alpha\rangle|^2\equiv|\mathcal{U}_{\beta\alpha}(t_f,t_i)|^2. \quad (19)$$

In our case, we identify $\mathcal{H}_0$ with the ULDM-independent contribution to Eq. (17), and denote $V(t)=V^{(1)}(t)+V^{(2)}(t)$ with

$$V^{(1)}(t)\equiv\frac{\phi_0}{2E}\tilde{m}\sin(m_\phi(t-t_0)), \quad (20)$$

$$V^{(2)}(t)\equiv\frac{\phi_0^2}{2E}y^\dagger y\sin^2(m_\phi(t-t_0)), \quad (21)$$

where we define $\tilde{m}\equiv m_\nu^\dagger\hat{y}+\hat{y}^\dagger m_\nu$. Then, the ULDM-independent probabilities $P^{(0)}_{\alpha\beta}$ are given by

$$P^{(0)}_{\alpha\beta}=|\mathcal{U}^{(0)}_{\beta\alpha}(t_f,t_i)|^2, \quad (22)$$

where

$$\mathcal{U}^{(0)}(t_f,t_i)=e^{-i\mathcal{H}_0(t_f-t_i)}. \quad (23)$$

As expected $\mathcal{U}^{(0)}(t_f,t_i)=\mathcal{U}^{(0)}(t_f-t_i)$. From this point onwards, we assume t_f-t_i corresponds to the propagation time over a distance L, i.e., $t_f-t_i\approx L$. Thus $\mathcal{U}^{(0)}$ and $P^{(0)}$ are functions of L alone, and do not vary with time. For the sake of brevity, moving forward we keep the L dependence implicit, and only explicitly note time dependencies. In addition, in the following we assume α and β are interaction eigenstates.

The leading order perturbation to the transition/survival probabilities is given by (no summation is implied on α, β)

$$P^{(1)}_{\alpha\beta}(t)=2\mathrm{Re}(\mathcal{U}^{(0)}_{\beta\alpha}\mathcal{U}^{(1)}_{\beta\alpha}(t)^*), \quad (24)$$

where

$$\mathcal{U}^{(1)}(t)=-i\int_{t-L}^{t}dt_1 e^{-i\mathcal{H}_0(t-t_1)}V^{(1)}(t_1)e^{-i\mathcal{H}_0(t_1-t+L)}$$
$$=-i\int_0^L dt_1 e^{-i\mathcal{H}_0(L-t_1)}V^{(1)}(t_1+t-L)e^{-i\mathcal{H}_0 t_1}. \quad (25)$$

Since $V^{(1)}$ given in Eq. (20) is sinusoidal, the integral is easily solved analytically, and we obtain

$$P^{(1)}_{\alpha\beta}(t)=\frac{2\phi_0}{E}\mathrm{Im}\left(U_{\beta k}U^*_{\alpha k}U^*_{\beta i}U_{\alpha j}\tilde{m}^*_{ij}e^{i\frac{(\Delta m^2_{jk}+\Delta m^2_{ik})L}{4E}}\kappa^*(t)_{ij}\right), \quad (26)$$

where the i, j, k indices correspond to the eigenstates of the ULDM-independent Hamiltonian $\mathcal{H}_0$ and U is the ULDM-independent PMNS matrix, namely, the transition matrix between the interaction eigenstates and the eigenstates of $\mathcal{H}_0$. Specifying the form of the ULDM couplings $\hat{y}_{ij}$ in the basis in which $\mathcal{H}_0$ is diagonal,

$$\tilde{m}_{ij}=(m^\dagger\hat{y}+\hat{y}^\dagger m)_{ij}=m_i\hat{y}_{ij}+\hat{y}^*_{ij}m_j$$
$$=\mathrm{Re}(\hat{y}_{ij})(m_i+m_j)+i\mathrm{Im}(\hat{y}_{ij})(m_i-m_j). \quad (27)$$

Last, $\kappa_{ij}(t)$ is complex, with phases that are only dynamical (CPC). Its real and imaginary parts are given by

$$\mathrm{Re}(\kappa_{ij})=\frac{\sin(m_\phi(t-\frac{L}{2}-t_0))}{\left(\frac{\Delta m^2_{ij}}{2E}\right)^2-m_\phi^2}\left(m_\phi\cos\frac{\Delta m^2_{ij}L}{4E}\sin\frac{m_\phi L}{2}\right.$$
$$\left.-\frac{\Delta m^2_{ij}}{2E}\sin\frac{\Delta m^2_{ij}L}{4E}\cos\frac{m_\phi L}{2}\right), \quad (28)$$

$$\mathrm{Im}(\kappa_{ij})=\frac{\cos(m_\phi(t-\frac{L}{2}-t_0))}{\left(\frac{\Delta m^2_{ij}}{2E}\right)^2-m_\phi^2}\left(\frac{\Delta m^2_{ij}}{2E}\cos\frac{\Delta m^2_{ij}L}{4E}\sin\frac{m_\phi L}{2}\right.$$
$$\left.-m_\phi\sin\frac{\Delta m^2_{ij}L}{4E}\cos\frac{m_\phi L}{2}\right). \quad (29)$$

From the temporal dependence of κ, and thus also of the neutrino probabilities, we see that simply adding up data points gathered over times larger than m_ϕ^{-1} would suppress

the effect due to averaging over different neutrino arrival times t. We therefore require time stamping the events with a minimal temporal resolution corresponding to $\sim 1/m_\phi$. While most previous analyses assumed the ULDM field to be constant during the propagation time L, we are interested in extending these results into the $m_\phi L \gtrsim 1$ region. For long baseline neutrino experiments, this is equivalent to

$$m_\phi \gtrsim 10^{-12}\ \text{eV}, \tag{30}$$

or

$$\tau_\phi \equiv \frac{2\pi}{m_\phi} \lesssim 1\ \text{ms}. \tag{31}$$

This timescale is much shorter than the typical time between events in any neutrino experiment. To study how to probe these time variations, we will use the unbinned Rayleigh periodogram, as will be explained in Sec. IV.

Note that in the limit $m_\phi L \to 0$, $2Em_\phi/\Delta m^2_{ij} \to 0$, we have $\text{Im}(\kappa_{ij})/\text{Re}(\kappa_{ij}) \to 0$ [$\text{Re}(\kappa_{ij})$ remains finite as $V(t) \propto \sin m_\phi(t-t_0)$]. Therefore, previous analyses that assumed the ULDM potential to be constant within the propagation time have effectively only taken into account effects that are associated with the real part of κ, which in that limit reduces to

$$\text{Re}(\kappa_{ij}) \approx -\frac{\sin(m_\phi(t-t_0))}{\frac{\Delta m^2_{ij}}{2E}} \sin\frac{\Delta m^2_{ij} L}{4E}. \tag{32}$$

In this limit, for ULDM couplings that are off-diagonal in the unperturbed mass basis, the result can be interpreted as following from the first-order correction to the diagonalizing matrix of the neutrino Hamiltonian in the interaction basis. Namely,

$$U_{\alpha k} \to \tilde{U}_{\alpha k}(t) = (UT^\dagger(t))_{\alpha k}, \tag{33}$$

where

$$T(t)_{ij} = \delta_{ij} + (1-\delta_{ij})\frac{\phi_0 \tilde{m}_{ij}}{\Delta m^2_{ij}} \sin(m_\phi(t-t_0)). \tag{34}$$

Note that in this limit, the new diagonalizing matrix $\tilde{U}$ is treated as constant within propagation, but changes its value for each measurement at time t.

To understand what happens when going beyond the constant potential limit, let us rewrite the EOM in the interaction basis as

$$i\partial_t \nu^I(t) = UT^\dagger(t)\mathcal{H}_D T(t) U^\dagger \nu^I(t) \approx UT^\dagger(t)\mathcal{H}_0 T(t) U^\dagger \nu^I(t), \tag{35}$$

where ν^I is given in the interaction basis and $\mathcal{H}_D$ is the instantaneously diagonal Hamiltonian, which to linear order in the ULDM perturbation is just $\mathcal{H}_0$. To solve the EOM, one may define

$$\tilde{\nu}(t) = \tilde{U}(t)^\dagger \nu^I(t) \tag{36}$$

and obtain

$$\begin{aligned} i\partial_t \tilde{\nu}(t) &= (\mathcal{H}_0 - i\tilde{U}(t)^\dagger \partial_t \tilde{U}(t))\tilde{\nu}(t) \\ &= (\mathcal{H}_0 - iT(t)\partial_t T(t)^\dagger)\tilde{\nu}(t). \end{aligned} \tag{37}$$

As the EOM is not diagonal due to the contributions coming from the time derivative of the Hamiltonian, one should in principle diagonalize the new effective Hamiltonian by another time dependent matrix, the derivative of which will again contribute to the Hamiltonian which should again be diagonalized, and so on. Keeping only the linear terms in the ULDM perturbation, this procedure will yield an infinite series in $\partial_t^{(n)} V^{(1)}_{ij}/(\Delta m^2_{ij})^n$, where $i \neq j$ and $V^{(1)}$ is defined in Eq. (20). The result of this series is the effective diagonalizing matrix

$$\tilde{U}(t) = U\tilde{T}^\dagger(t), \tag{38}$$

with

$$\begin{aligned} \tilde{T}_{ij}(t) = \delta_{ij} &+ (1-\delta_{ij})\frac{\phi_0 \tilde{m}_{ij}}{\Delta m^2_{ij}} \\ &\times \sum_{n=0}^{\infty} i^n \left(\frac{2E}{\Delta m^2_{ij}}\right)^n \partial_t^{(n)} \sin(m_\phi(t-t_0)). \end{aligned} \tag{39}$$

Since our potential is harmonic, we can easily sum all the contributions up to infinity and obtain

$$\begin{aligned} \tilde{T}_{ij}(t) = \delta_{ij} &+ (1-\delta_{ij})\frac{\phi_0 \tilde{m}_{ij}}{\Delta m^2_{ij}} \frac{1}{1-\left(\frac{2Em_\phi}{\Delta m^2_{ij}}\right)^2} \\ &\times \left(\sin(m_\phi(t-t_0)) + i\frac{2Em_\phi}{\Delta m^2_{ij}}\cos(m_\phi(t-t_0))\right). \end{aligned} \tag{40}$$

Therefore, the neutrino flavor probabilities are given by taking the zeroth and first-order terms in $\phi_0 \tilde{m}_{ij}/\Delta m^2_{ij}$ of

$$P_{\alpha\beta}(t) \approx \tilde{U}_{\beta k}(t)\tilde{U}^*_{\alpha k}(t-L)\tilde{U}^*_{\beta i}(t)\tilde{U}_{\alpha i}(t-L)e^{-i\frac{\Delta m^2_{kl} L}{2E}}. \tag{41}$$

In the next subsections, we describe the full ULDM effects in three generations, first considering CPC observables in Sec. III B, and then CPV phenomena in Sec. III C. Note, however, that the expressions above are completely generic for any number of generations, provided the indices

are appropriately summed. The probabilities for the two-generation case are presented in Appendix A.

B. CPC effects

In the standard case with three neutrino generations, the neutrino probabilities in three generations are given by

$$P^{(0)}_{\alpha\beta} = U_{\beta k}U^*_{\alpha k}U^*_{\beta i}U_{\alpha i}e^{-i\frac{\Delta m^2_{ki}L}{2E}}. \tag{42}$$

The CPC part of this probability is given by averaging over neutrinos and antineutrinos:

$$\Sigma P^{(0)}_{\alpha\beta} \equiv \frac{1}{2}(P^{(0)}_{\alpha\beta} + P^{(0)}_{\bar\alpha\bar\beta}) = \mathrm{Re}(U_{\beta k}U^*_{\alpha k}U^*_{\beta i}U_{\alpha i})\cos\left(\frac{\Delta m^2_{ki}L}{2E}\right). \tag{43}$$

We now discuss the first-order corrections from ULDM to CPC neutrino probabilities. From Eq. (26), we find CPC contributions to be associated with the real parts of the complex matrices U and $\hat{y}$. Let us denote these contributions by $\Sigma P^{(1)}_{\alpha\beta}$:

$$\Sigma P^{(1)}_{\alpha\beta} \equiv \frac{1}{2}(P^{(1)}_{\alpha\beta} + P^{(1)}_{\bar\alpha\bar\beta}) = \frac{2\phi_0}{E}\mathrm{Re}(U_{\beta k}U^*_{\alpha k}U^*_{\beta i}U_{\alpha j}\tilde{m}^*_{ij}) \times \mathrm{Im}\left(e^{i\frac{(\Delta m^2_{jk}+\Delta m^2_{ik})L}{4E}}\kappa^*(t)_{ij}\right). \tag{44}$$

In three generations, for diagonal couplings $\hat{y}_{ii}$, both $\tilde{m}_{ii}$ and κ_{ii} are real, and thus for a specific i, specific $j \neq k \neq i$ and any α, β,

$$\Sigma P^{(1)}_{\alpha\beta}(t) = -\sin\left(m_\phi\left(t - \frac{L}{2} - t_0\right)\right)\sin\left(\frac{m_\phi L}{2}\right)\frac{2\tilde{m}_{ii}\phi_0}{Em_\phi} \times \left(\mathrm{Re}(U_{\beta k}U^*_{\alpha k}U^*_{\beta i}U_{\alpha i})\sin\left(\frac{\Delta m^2_{ik}L}{2E}\right) + \mathrm{Re}(U_{\beta j}U^*_{\alpha j}U^*_{\beta i}U_{\alpha i})\sin\left(\frac{\Delta m^2_{ij}L}{2E}\right)\right). \tag{45}$$

This result is nothing but an effective, time dependent shift of the neutrino mass differences Δm^2_{ij},

$$\Delta m^2_{ij} \to \Delta m^2_{ij} + \frac{2m_i\phi_0\hat{y}_{ii}}{L}\int_{t-L}^{t}\sin(m_\phi(t_1 - t_0))dt_1. \tag{46}$$

Effects of this sort have already been quite thoroughly discussed in previous works such as [1,2,6,7].

For off-diagonal couplings $\hat{y}_{ij}$, with $i \neq j \neq k$ transition probabilities ($\alpha \neq \beta$) are modified by

$$\begin{aligned}\Sigma P^{(1)}_{\alpha\beta} = {} & \frac{4\phi_0}{E}\mathrm{Im}(\kappa^*(t)_{ij})\mathrm{Re}(U_{\beta k}U^*_{\alpha k}(U^*_{\beta i}U_{\alpha j}\tilde{m}^*_{ij} - U^*_{\beta j}U_{\alpha i}\tilde{m}_{ij}))\sin\frac{\Delta m^2_{ik}L}{4E}\sin\frac{\Delta m^2_{kj}L}{4E} \\ & + \frac{4\phi_0}{E}\mathrm{Re}(\kappa^*(t)_{ij})\left[\mathrm{Re}(U_{\beta j}U^*_{\alpha j}(U^*_{\beta i}U_{\alpha j}\tilde{m}^*_{ij} + U^*_{\beta j}U_{\alpha i}\tilde{m}_{ij}))\sin\frac{\Delta m^2_{kj}L}{4E}\cos\frac{\Delta m^2_{ki}L}{4E}\right. \\ & \left. + \mathrm{Re}(U_{\beta i}U^*_{\alpha i}(U^*_{\beta i}U_{\alpha j}\tilde{m}^*_{ij} + U^*_{\beta j}U_{\alpha i}\tilde{m}_{ij}))\sin\frac{\Delta m^2_{ki}L}{4E}\cos\frac{\Delta m^2_{kj}L}{4E}\right],\end{aligned} \tag{47}$$

and survival probabilities ($\alpha = \beta$) by

$$\Sigma P^{(1)}_{\alpha\alpha} = \frac{4\phi_0}{E}\mathrm{Re}(\kappa(t)_{ij})\mathrm{Re}(U^*_{\alpha i}U_{\alpha j}\tilde{m}^*_{ij}) \times \left[(2|U_{\alpha j}|^2 - 1)\sin\frac{\Delta m^2_{kj}L}{4E}\cos\frac{\Delta m^2_{ki}L}{4E} + (2|U_{\alpha i}|^2 - 1)\sin\frac{\Delta m^2_{ki}L}{4E}\cos\frac{\Delta m^2_{kj}L}{4E}\right]. \tag{48}$$

As mentioned, previous analyses considered the constant ULDM limit, in which κ_{ij} is strictly real, and given by Eq. (32). In this case, one may interpret the first-order corrections as simple modifications to the PMNS matrix $U \to \tilde{U}$ as in Eqs. (33) and (34). However, moving away from this limit, we may no longer use the constant $\tilde{U}$ description. This leads to the different energy dependence of the result associated with $\mathrm{Im}(\kappa)$ and with the nonzeroth order terms in $2Em_\phi/(\Delta m^2_{ij})$ appearing in $\mathrm{Re}(\kappa)$.

C. CPV effects

CPV is realized in vacuum in the three neutrino picture. The difference between the neutrino and antineutrino transition probability is given by

$$\Delta P^{\text{standard}}_{\alpha\beta} = 4\sum_{i>j}\text{Im}(U^*_{\alpha i}U_{\beta i}U_{\alpha j}U^*_{\beta j})\sin\frac{\Delta m^2_{ij}L}{2E}$$
$$= 16J\sin\frac{\Delta m^2_{31}L}{4E}\sin\frac{\Delta m^2_{21}L}{4E}\sin\frac{\Delta m^2_{32}L}{4E}\sum_\gamma \varepsilon_{\alpha\beta\gamma}, \tag{49}$$

where the $\varepsilon_{\alpha\beta\gamma}$ is the three-dimensional Levi-Civita tensor and J is the Jarlskog invariant:

$$J = \cos\theta_{13}\sin 2\theta_{12}\sin 2\theta_{13}\sin 2\theta_{23}\sin\delta_{\text{CP}}. \tag{50}$$

Notice that CPV vanishes if we set any Δm^2_{ij} to be zero, which will result in an effective two-neutrino picture. We therefore name this source of CPV the "3-ν CPV."

Let us now discuss CPV in the presence of ULDM interactions with neutrinos. From Eq. (26), we find the CPV part of neutrino probabilities, i.e., the difference between neutrino and antineutrino probabilities $\Delta P^{(1)}_{\alpha\beta}$ to be

$$\Delta P^{(1)}_{\alpha\beta} \equiv P^{(1)}_{\alpha\beta} - P^{(1)}_{\bar\alpha\bar\beta}$$
$$= -\frac{4\phi_0}{E}\sum_{i,j,k}\text{Im}(U^*_{\beta k}U_{\alpha k}U_{\beta i}U^*_{\alpha j}\tilde m_{ij})$$
$$\times\text{Re}\left(e^{i\frac{(\Delta m^2_{jk}+\Delta m^2_{ik})L}{4E}}{\kappa_{ij}}^*\right). \tag{51}$$

Previous works have assumed the neutrino Hamiltonian to be constant throughout propagation, and thus the ULDM effects were thought of as slow temporal modulations of the standard neutrino oscillation parameters. In this limit, as mentioned, κ_{ij} is strictly real, and CPV can be interpreted as a slow variation of the standard CPV result [6]. Explicitly, in three generations, the contribution of the real part of κ for $i\neq j\neq k$ and $\alpha\neq\beta$, for a specific $\hat y_{ij}=\hat y_{ji}\neq 0$ is

$$\Delta P^{(1)}_{\alpha\beta} = -8\frac{\phi_0}{E}\text{Re}(\kappa_{ij})\sin\frac{\Delta m^2_{jk}L}{4E}\sin\frac{\Delta m^2_{ik}L}{4E}$$
$$\times\text{Im}(U^*_{\beta k}U_{\alpha k}(U_{\beta i}U^*_{\alpha j}\tilde m_{ij}+U_{\beta j}U^*_{\alpha i}\tilde m^*_{ij})), \tag{52}$$

which yields in the $m_\phi L\to 0$, $2Em_\phi/\Delta m^2_{ij}\to 0$, $V(t)\propto\sin m_\phi t$ limit

$$\Delta P^{(1)}_{\alpha\beta} \approx -16\frac{\phi_0}{\Delta m^2_{ij}}\sin\left(m_\phi\left(t-\frac{L}{2}-t_0\right)\right)\cos\frac{m_\phi L}{2}$$
$$\times\sin\frac{\Delta m^2_{ij}L}{4E}\sin\frac{\Delta m^2_{jk}L}{4E}\sin\frac{\Delta m^2_{ik}L}{4E}$$
$$\times\text{Im}(U^*_{\beta k}U_{\alpha k}(U_{\beta i}U^*_{\alpha j}\tilde m_{ij}+U_{\beta j}U^*_{\alpha i}\tilde m^*_{ij})). \tag{53}$$

Since we keep only first-order terms in the ULDM couplings, which here we assume to be off-diagonal in the ULDM-independent mass basis, one may interpret this result as the effect of the first-order correction to the standard Jarlskog invariant.

For diagonal couplings $\hat y_{ii}$, both $\tilde m_{ii}$ and κ_{ii} are real, and thus

$$\Delta P^{(1)}_{\alpha\beta}(t) = -\frac{4\tilde m_{ii}\phi_0}{Em_\phi}\sin\left(m_\phi\left(t-\frac{L}{2}-t_0\right)\right)\sin\left(\frac{m_\phi L}{2}\right)$$
$$\times\text{Im}(U_{\beta j}U^*_{\alpha j}U^*_{\beta i}U_{\alpha i})\sin\left(\frac{(\Delta m^2_{ik}+\Delta m^2_{ij})L}{4E}\right)$$
$$\times\sin\left(\frac{\Delta m^2_{kj}L}{4E}\right). \tag{54}$$

This CPV term is, of course, proportional to J, as only the real part of diagonal couplings affects the neutrino Hamiltonian. This term is simply a correction to the mass differences of the neutrinos coming from the ULDM coupling, as shown in Eq. (46).

For off-diagonal couplings, stepping away from the $m_\phi\to 0$ limit, we should also consider the contribution of the imaginary part of κ,

$$\Delta P^{(1)}_{\alpha\beta} = 4\text{Im}(\kappa_{ij})\sum_{i,j,k}\text{Im}(U^*_{\beta k}U_{\alpha k}U_{\beta i}U^*_{\alpha j}\tilde m_{ij})$$
$$\times\sin\left(\frac{(\Delta m^2_{jk}+\Delta m^2_{ik})L}{4E}\right). \tag{55}$$

For $i\neq j\neq k$ and $\alpha\neq\beta$, for a specific $\hat y_{ij}=\hat y_{ji}\neq 0$, it becomes

$$\Delta P^{(1)}_{\alpha\beta} = 8\text{Im}(\kappa_{ij})\Big[\text{Im}(U^*_{\beta i}U_{\alpha i}(U_{\beta j}U^*_{\alpha i}\tilde m^*_{ij}-U_{\beta i}U^*_{\alpha j}\tilde m_{ij}))\sin\frac{\Delta m^2_{ik}L}{4E}\cos\frac{\Delta m^2_{jk}L}{4E}$$
$$+\text{Im}(U^*_{\beta j}U_{\alpha j}(U_{\beta j}U^*_{\alpha i}\tilde m^*_{ij}-U_{\beta i}U^*_{\alpha j}\tilde m_{ij}))\cos\frac{\Delta m^2_{ik}L}{4E}\sin\frac{\Delta m^2_{jk}L}{4E}\Big]. \tag{56}$$

This expression is fundamentally different from the 3-ν CPV effect, as it "contains" the 2-ν CPV effect we discussed in Sec. II [see Eq. (16)]. This can be seen in three distinct ways, all pointing to cases in which there would be no CPV in the constant ULDM potential limit.

First, note that Eq. (53) vanishes for $U^*_{\beta k}U_{\alpha k}=0$, namely, when the projection of the mass eigenstate not coupled to the ULDM on either the outgoing or the incoming interaction eigenstates vanishes. This case corresponds to an effective $J=0$. However, taking this limit for Eq. (56), we obtain

$$\Delta P^{(1)}_{\alpha\beta} = 8\mathrm{Im}(\kappa_{ij})\mathrm{Im}(U^*_{\beta i}U_{\alpha i}(U_{\beta j}U^*_{\alpha i}\tilde{m}^*_{ij} - U_{\beta i}U^*_{\alpha j}\tilde{m}_{ij})) \times \sin\frac{\Delta m^2_{ij}L}{4E}. \tag{57}$$

This expression does not vanish generically. Specifically, if say only $U_{\alpha k}=0$, then unitarity implies $|U_{\alpha i}|^2+|U_{\alpha j}|^2=1$, and we may denote $|U_{\alpha i}|^2\equiv\sin^2\theta_\alpha$ and obtain

$$\Delta P^{(1)}_{\alpha\beta} = 16\cos 2\theta_\alpha \mathrm{Im}(\kappa_{ij})\mathrm{Im}(U_{\beta i}U^*_{\beta j}\tilde{m}_{ij})\sin\frac{\Delta m^2_{ij}L}{4E}. \tag{58}$$

This effect is indeed the result of the two-generations-like effect, and thus does not vanish.

Second, as explained above, we expect the standard CPV effect in three generations to vanish when any of the mass differences Δm^2_{ij} vanish. Indeed, the standard CPV in Eq. (49) vanishes at this limit, as well as the constant-ULDM CPV in Eq. (53) when considering a specific off-diagonal $\hat{y}_{ij}$, and setting $\Delta m^2_{jk}=0$, for $k\neq i\neq j$. However, at this limit, Eq. (56) yields a nonzero result and reads

$$\Delta P^{(1)}_{\alpha\beta} = 8\mathrm{Im}(\kappa_{ij})\mathrm{Im}(U^*_{\beta i}U_{\alpha i}(U_{\beta j}U^*_{\alpha i}\tilde{m}^*_{ij} - U_{\beta i}U^*_{\alpha j}\tilde{m}_{ij})) \times \sin\frac{\Delta m^2_{ij}L}{4E}, \tag{59}$$

exactly as in the $U^*_{\beta k}U_{\alpha k}=0$ case (however, here we do not assume a specific structure for U). Given the known hierarchy in the neutrino mass differences, $\Delta m^2_{12}\ll\Delta m^2_{31},\Delta m^2_{32}$, we then expect that the new 2-ν CPV effect resulting from $\hat{y}_{31}$ or $\hat{y}_{32}$ would dominate over the constant ULDM CPV roughly for $m_\phi\gtrsim\Delta m^2_{12}/(2E)$. Note that if the neutrinos coupled to the ULDM are degenerate in the unperturbed system, i.e., $\hat{y}_{ij}\neq 0$ for $\Delta m^2_{ij}L/(4E)\to 0$, the constant ULDM limit $m_\phi L\to 0$ yields a nonzero CPV, as $\mathrm{Re}(\kappa_{ij})\to\sin(m_\phi(t-t_0))L/2$. This corresponds to a leading order effective mass difference induced by the ULDM potential. In this limit, we obtain $\mathrm{Im}(\kappa_{ij})\propto L^3 m_\phi\Delta m^2_{ij}/(4E)$, and thus the 2-$\nu$ CPV effect is expected to be subdominant to the constant ULDM effect.

Finally, note that standard CPV does not affect survival probabilities. Accordingly, the constant-ULDM CPV in Eq. (53) is also zero for $\alpha=\beta$. The new CPV effect we found in Eq. (55) for $\alpha=\beta$ does not vanish generically and is given for a specific $\hat{y}_{ij}=\hat{y}_{ji}\neq 0$ with $i\neq j\neq k$ by

$$\Delta P^{(1)}_{\alpha\alpha} = -8\mathrm{Im}(\kappa_{ij})\mathrm{Im}(\tilde{m}_{ij}U_{\alpha i}U^*_{\alpha j}) \times\left((2|U_{\alpha j}|^2+1)\sin\left(\frac{\Delta m^2_{jk}L}{4E}\right)\cos\left(\frac{\Delta m^2_{ik}L}{4E}\right) + (2|U_{\alpha i}|^2+1)\cos\left(\frac{\Delta m^2_{jk}L}{4E}\right)\sin\left(\frac{\Delta m^2_{ik}L}{4E}\right)\right). \tag{60}$$

Therefore, even experiments measuring only survival probabilities would be sensitive to CPV ULDM-neutrino couplings. This is a completely new prediction resulting from our analysis, considering the time variations of the Hamiltonian within the neutrino propagation time.

IV. EXPERIMENTAL IMPLICATIONS—RAYLEIGH PERIODOGRAM

In Sec. III, we introduced analytical expressions for the first-order modifications to neutrino probabilities resulting from ULDM-neutrino interactions. We are interested in devising a method for detecting these modifications in neutrino oscillations experiments. As the effects we found are time dependent, characterized by simple oscillatory functions with periods $\tau_\phi=2\pi/m_\phi$, we are essentially interested in measuring the spectral power of the neutrino probabilities at an angular frequency corresponding to m_ϕ.

Consider the following timescales relevant for neutrino oscillation experiments:

(1) τ_e: The running time of the experiment.
(2) $\tau_s=\frac{\tau_e}{N_\nu}$: The average spacing between events, where N_ν is the total number of measured events.
(3) τ_r: The resolution of the event timing. While in practice the effective resolution could be set by different sources of temporal uncertainty (e.g., beam spread), we will refer to it as the "clock" resolution.

We notice the following hierarchy between the timescales:

$$\tau_r\ll\tau_s\ll\tau_e. \tag{61}$$

Since the frequencies we are interested in are determined by τ_ϕ, one would naively assume that the experimental sensitivity to ULDM masses $m_\phi\gtrsim 2/\tau_s$ would be suppressed, as the statistical uncertainty on the neutrino probability binned over the corresponding τ_ϕ would be quite large, due to a small number of events expected to occur within that period. However, as we will now show, the true limiting factor, in terms of the experimental sensitivity, is rather the effective clock resolution τ_r, which is much smaller than τ_s.

To understand this, first recall that the events are inherently binned over times τ_r, while τ_s is not associated with some instrumental resolution, and binning over it is completely artificial and is done postmeasurement. Let us then use the full data, given as the number of neutrinos of a

certain flavor detected at a sequence of $N_t = \tau_e/\tau_r$ clock ticks, each with short duration τ_r. Since $\tau_r \ll \tau_s$, we ignore the possibility that two neutrinos might be detected during τ_r, and define the following power spectrum:

$$z(f) = \frac{2}{N_\nu}\left(\left[\sum_{n=1}^{N_t} h(t_n)\cos(2\pi f t_n)\right]^2 + \left[\sum_{n=1}^{N_t} h(t_n)\sin(2\pi f t_n)\right]^2\right), \tag{62}$$

with

$$h(t_i) = \begin{cases} 1 & \text{event detected,} \\ 0 & \text{no event detected.} \end{cases} \tag{63}$$

This definition gives us the well-known Rayleigh power spectrum

$$z(f) = \frac{2}{N_\nu}\left(\left[\sum_{n=1}^{N_\nu}\cos(2\pi f t_n)\right]^2 + \left[\sum_{n=1}^{N_\nu}\sin(2\pi f t_n)\right]^2\right). \tag{64}$$

Notice that the summation now is over the neutrino events instead of over time bins. For a list of events detected in a time series $\{t_n\}$, we calculate the power spectrum z, which is an analytic function of the probed frequencies f. For $\{t_n\}$ uniformly random distributed between $0 < t_n < \tau_e$, the sum of sines and the sum of cosines in Eq. (64) are each normally distributed with the mean value of zero and standard deviation of $\sqrt{N_\nu/2}$. Thus $z(f)$, being their appropriately normalized sum of squares, is Chi-squared distributed with 2 degrees of freedom, which is simply an exponential distribution of z. This means, under the background only hypothesis, that if we consider a specific frequency f' and calculate its power $z(f')$, its probability to be higher than some value Z is independent of the frequency f' (assuming $f' \gtrsim 1/\tau_e$ and no other spectral noise sources) and is given by

$$p(z > Z) = \int_Z^\infty \frac{1}{2} e^{-z/2} dz = e^{-Z/2}. \tag{65}$$

Let us estimate the signal in case of a temporal modulation of the neutrino probability. The probability of detecting a neutrino of some flavor at time t_i in an energy bin $[E_{j,\min}, E_{j,\max}]$ is given by

$$P(h(t_i, E_j) = 1) = \int_{E_{j,\min}}^{E_{j,\max}} \int_{t_i-\tau_r/2}^{t_i+\tau_r/2} dt dE F(E) P(E,t), \tag{66}$$

where F is the unoscillated neutrino flux; i.e., the flux that would have reached the detector had all the produced neutrinos oscillated into the flavor in question

$$F(E) = \frac{dN_{\text{unoscillated}}}{dE dt}, \tag{67}$$

and $P(E,t)$ is the oscillation probability given by

$$P(E,t) = P^{(0)}(E) + P^{(1)}(E,t), \tag{68}$$

with $P^{(0)}$ and $P^{(1)}$ given in Eqs. (22) and (24). The total number of events collected from different energy bins over the entire duration of the experiment τ_e, assuming the ULDM modification to the probability is very small, is then

$$N_\nu \approx \int_{E_{\min}}^{E_{\max}} \int_0^{\tau_e} dt dE F(E) P^{(0)}(E) = \tau_e \int_{E_{\min}}^{E_{\max}} dE F(E) P^{(0)}(E). \tag{69}$$

Similarly, one may define the corresponding number of events associated with the small ULDM probability

$$N^{(1)}_{\nu,s} = \tau_e \int_{E_{\min}}^{E_{\max}} dE F(E) P^{(1)}_s(E), \tag{70}$$

$$N^{(1)}_{\nu,c} = \tau_e \int_{E_{\min}}^{E_{\max}} dE F(E) P^{(1)}_c(E), \tag{71}$$

where P_s and P_c can be read off from

$$P^{(1)}(E,t) = P^{(1)}_s(E)\sin(m_\phi t) + P^{(1)}_c(E)\cos(m_\phi t). \tag{72}$$

To identify $P^{(1)}_s(E)$ and $P^{(1)}_c(E)$, note that the imaginary and real components of κ_{ij} determine the time dependence of $P^{(1)}$, as can be seen in Eqs. (28) and (29). Since $\mathrm{Re}(\kappa)$ and $\mathrm{Im}(\kappa)$ are orthogonal in time, but have the same frequency, $P^{(1)}$ can be written as

$$P^{(1)} = a\sin(m_\phi(t - L/2 - t_0)) + b\cos(m_\phi(t - L/2 - t_0)), \tag{73}$$

and thus

$$P^{(1)}_s = a\cos(m_\phi(L/2 + t_0)) + b\sin(m_\phi(L/2 + t_0)), \tag{74}$$

$$P^{(1)}_c = -a\sin(m_\phi(L/2 + t_0)) + b\cos(m_\phi(L/2 + t_0)). \tag{75}$$

We may now calculate the expected value of $z(f)$ at $f = m_\phi/(2\pi)$ in the presence of a ULDM, with mass m_ϕ, interacting with neutrinos.[2] One can show (see Appendix B) that for $m_\phi \lesssim 2/\tau_r$,

$$\left\langle \left[\sum_{i=1}^{N_\nu} \sin(2\pi t_i f)\right]^2 \right\rangle = \frac{N_\nu}{2} + \frac{(N_s^{(1)})^2}{4}, \tag{76}$$

$$\left\langle \left[\sum_{i=1}^{N_\nu} \cos(2\pi t_i f)\right]^2 \right\rangle = \frac{N_\nu}{2} + \frac{(N_c^{(1)})^2}{4}, \tag{77}$$

and thus

$$\begin{aligned}\langle z(f)\rangle &= \frac{2}{N_\nu}\left[\left\langle \left[\sum_{i=1}^{N_\nu} \sin(2\pi t_i f)\right]^2 \right\rangle \right. \\ &\quad \left. + \left\langle \left[\sum_{i=1}^{N_\nu} \cos(2\pi t_i f)\right]^2 \right\rangle\right] \\ &= 2 + \frac{(N_s^{(1)})^2 + (N_c^{(1)})^2}{2N_\nu}.\end{aligned} \tag{78}$$

Note a few key points regarding the above result:

(i) The expected sensitivity to a ULDM coupling $\hat{y}$ improves with the square root of the (unoscillated) neutrino flux of the experiment $\sqrt{F}$, and decreases as the square root of the expected vacuum oscillation probability $\sqrt{P^{(0)}}$.

(ii) Assuming the ULDM perturbation is coherent throughout the experimental time, the sensitivity to $\hat{y}$ improves as $\sqrt{\tau_e}$. For a coherence time τ_c satisfying $L, \tau_r < \tau_c < \tau_e$, the sensitivity to $\hat{y}$ would follow $\sqrt{\tau_e}\left(\frac{\tau_c}{\tau_e}\right)^{\frac{1}{4}}$. While our results were derived assuming $\tau_c \gtrsim \tau_r, L$, it is possible to derive the appropriate expressions for $\tau_c < L, \tau_r$ by statistically averaging over the ULDM phase [either in determining $P^{(1)}$ from the Dyson integral over L in Eq. (25) or in the integral over τ_r in Eq. (66)], which might significantly suppress the linear contributions to the neutrino probabilities.

(iii) As stated, since the distribution of $z(f)$ under the null hypothesis is frequency independent, the expected sensitivity of the experiment for different ULDM masses is completely determined by the mass dependence of $P^{(1)}$, assuming $m_\phi \lesssim 2/\tau_r$ and $\tau_c \gtrsim \tau_e$ (or mass-independent coherence times). If the ULDM coherence time is determined by $\tau_c = 2\pi/(m_\phi\beta^2)$ with the viral velocity $\beta \approx 10^{-3}$, then for $m_\phi > 2\pi/(\tau_e\beta^2)$ one can think of $P^{(1)}$ as being effectively suppressed by an additional factor of $\left(\frac{2\pi}{\tau_e m_\phi \beta^2}\right)^{\frac{1}{4}}$. For $m_\phi > 2/\tau_r$, the integration over time τ_r in Eq. (66) would yield an effective additional $2/(m_\phi\tau_r)$ suppression to $P^{(1)}$. Also note that our result coincides with the result obtained by previous analyses assuming $\tau_s < \tau_\phi$ if one sets $\tau_r = \tau_s$. Therefore, compared to previous analyses, the Rayleigh method would yield bounds on the couplings of ULDM of masses $2/\tau_r > m_\phi > 2/\tau_s$ that are stronger by $m_\phi\tau_s$, and bounds that are stronger by τ_s/τ_r for $m_\phi > 2/\tau_r$.

(iv) While the ULDM phase (denoted by $m_\phi t_0$) affects the sum of cosines and the sum of sines in Eqs. (77) and (76), respectively, it does not affect $z(f)$, as they are added in quadrature. Namely, the calculation of $z(f)$ does not require a knowledge of the ULDM phase, and the phase of the cosines and sines used for it may be chosen arbitrarily. Consequently, to calculate the expected bounds, one could treat the time-independent factors associated with $\mathrm{Re}(\kappa_{ij})$ and $\mathrm{Im}(\kappa_{ij})$ separately, as they will be added in quadrature. Of course, scanning over the phase and examining the sum of cosines and sum of sines independently would allow recovering the ULDM phase information.

(v) While in our calculation we used the simple modulation function $h(t_i)$ in Eq. (63), one may use other choices for h in order to isolate or amplify specific properties of the signal. Specifically, assigning $h(t_i) = h(E)$ would effectively set a different, energy-dependent, weight for the neutrino events, which could be helpful, for example, in recovering energy-dependent highly oscillatory components of the signal. Another useful choice could be made to isolate either the CPC or the CPV probabilities in an experiment that allows for detecting both neutrinos and antineutrinos, as

$$h_\pm(t_i) = \begin{cases} 1/n_\nu & \nu \text{ event detected}, \\ \pm 1/n_{\bar{\nu}} & \bar{\nu} \text{ event detected}, \\ 0 & \text{no event detected}, \end{cases} \tag{79}$$

where n_ν is the total number of neutrinos detected and $n_{\bar{\nu}}$ is the total number of antineutrinos detected.

[2]We do not specify the range and resolution of frequencies at which a peak in the Rayleigh spectrum is searched for, as there is no clear recipe for determining them. One can scan frequencies as small as $\sim\tau_e^{-1}$, and as large as τ_r^{-1}, since the effect is suppressed for frequencies higher than that. Typically, the resolution of the scan would be approximately $\sim\tau_e^{-1}$, as this is the width of the features in $z(f)$. However, the authors of [19], for example, chose to oversample with a higher resolution. This comes at the cost of a more significant look-elsewhere effect [20], which reduces the confidence level of the signal. Since this effect is mainly determined by the number of frequencies one scans, a number which depends neither on the experiment nor on the ULDM parameters, we did not include it in the analyses in this paper.

Generally speaking, for any choice of a modulation function $h(\phi)$ which is time independent (let it be a function of the neutrino energy, flavor, lepton number, etc.), we may define

$$\tilde{r}(f) = \left(\left[\sum_{i=1}^{N_\nu} h(\phi_i) \sin(2\pi t_i f) \right]^2 + \left[\sum_{i=1}^{N_\nu} h(\phi_i) \cos(2\pi t_i f) \right]^2 \right). \quad (80)$$

Then, the modified Rayleigh score

$$\tilde{z}(f) = \frac{2}{\tilde{N}_\nu^0} \tilde{r}(f) \quad (81)$$

is χ_2^2 distributed, and in the presence of a signal its expectation value is

$$\langle \tilde{z}(f) \rangle = 2 + \frac{(\tilde{N}_s^{(1)})^2 + (\tilde{N}_c^{(1)})^2}{2\tilde{N}_\nu^0}, \quad (82)$$

with

$$\tilde{N}_\nu^0 = \left\langle \sum_{\text{bkg}} h^2 \right\rangle = \tau_e \int_{E_{\min}}^{E_{\max}} \int_\phi \frac{dN}{dE dt d\phi} P^{(0)} h^2 d\phi dE, \quad (83)$$

$$\tilde{N}_{\nu,s}^{(1)} = \left\langle \sum_{\text{s}} h \right\rangle = \tau_e \int_{E_{\min}}^{E_{\max}} \int_\phi \frac{dN}{dE dt d\phi} P_s^{(1)} h d\phi dE, \quad (84)$$

$$\tilde{N}_{\nu,c}^{(1)} = \left\langle \sum_{\text{c}} h \right\rangle = \tau_e \int_{E_{\min}}^{E_{\max}} \int_\phi \frac{dN}{dE dt d\phi} P_c^{(1)} h d\phi dE. \quad (85)$$

Then, concretely, for $h_\pm$ one would obtain

$$\langle \tilde{z}(f) \rangle_\pm \approx 2 + \frac{(\epsilon_s^\pm)^2 + (\epsilon_c^\pm)^2}{2\left(\frac{1}{n_\nu} + \frac{1}{n_{\bar{\nu}}}\right)}, \quad (86)$$

with

$$\epsilon_{s,c}^+ = \frac{\int_{E_{\min}}^{E_{\max}} dE F(E) 2\Sigma P_{s,c}^{(1)}(E)}{\int_{E_{\min}}^{E_{\max}} dE F(E) P^{(0)}(E)}, \quad (87)$$

$$\epsilon_{s,c}^- = \frac{\int_{E_{\min}}^{E_{\max}} dE F(E) \Delta P_{s,c}^{(1)}(E)}{\int_{E_{\min}}^{E_{\max}} dE F(E) P^{(0)}(E)}, \quad (88)$$

with $\Sigma P^{(1)}$ and $\Delta P^{(1)}$ defined in Eqs. (44) and (51), respectively.

V. CURRENT AND FUTURE-PROJECTED BOUNDS

In this section we study the sensitivity of various neutrino oscillation experiments to the ULDM modulation amplitude using the Rayleigh periodogram. We derive bounds on the neutrino-ULDM couplings from existing experiments which have already looked for time modulations in neutrino survival and transition probabilities, and projected sensitivities for future experiments. We do not use Monte Carlo simulations, but use the scaling that we derived for the expectation value of the magnitude of the Rayleigh spectrum peak at the modulation frequency in Eq. (78), with the parameters of the experiment and of the model. When calculating the height of the peak, we assumed that the ULDM modulation amplitude is predominantly affected by one entry of the $\hat{y}$ matrix at a time. We also provide a separate analysis for the real and imaginary components of the off-diagonal entries of $\hat{y}$, assuming $\delta_{CP} = 0$. Note that in our calculations we assumed a normal hierarchy, and that $m_1 = 0$. The latter assumption can be relaxed by re-identifying $\text{Im}(y_{1i}) \to (m_i - m_1)\text{Im}(y_{1i})/m_i$, $\text{Re}(y_{1i}) \to (m_i + m_1)\text{Re}(y_{1i})/m_i$ for the off-diagonal couplings, and $y_{22} \to y_{22} - m_1 y_{11}/m_2$, $y_{33} \to y_{33} - m_1 y_{11}/m_3$ for the diagonal ones. For the projected sensitivities, we find the curve in parameter space $\hat{y}(m_\phi)$ for which the peak is expected to match the 95% percentile of the χ_2^2 distribution, characterizing the background (corresponding to a CL $= 0.95$). The corresponding bounds in terms of the ULDM parameters are shown in Fig. 1.

A. Current bounds

1. Daya-Bay

The Daya Bay experiment collects $\bar{\nu}_e$ events from nearby reactors which are approximately 800 meters away from the detector. The collaboration has searched for time dependent modulations of the survival probability $P_{\bar{e}\bar{e}}$, for frequencies between 5.9×10^{-5}/sidereal hour to 0.5/sidereal hour, and found no significant evidence [22]. We plot in Fig. 1 the ULDM couplings corresponding to an expected sensitivity at CL $= 0.95$, assuming 621 days of data taking, with a total of 800 unoscillated events per day [23].

2. Solar experiments—SNO

The Super-K and SNO experiments collect solar ν_e with event rates of 15/day [24] and 10/day [25], respectively. Because of the Mikheyev-Smirnov-Wolfenstein effect, neutrinos with energy larger than ~1 MeV leave the sun as the ν_2 mass states. Therefore, their survival probability does not oscillate with propagation and is given by $P_{2e}^0 = |U_{e2}|^2 \approx \sin^2\theta_{12}$. This means that up to day/night

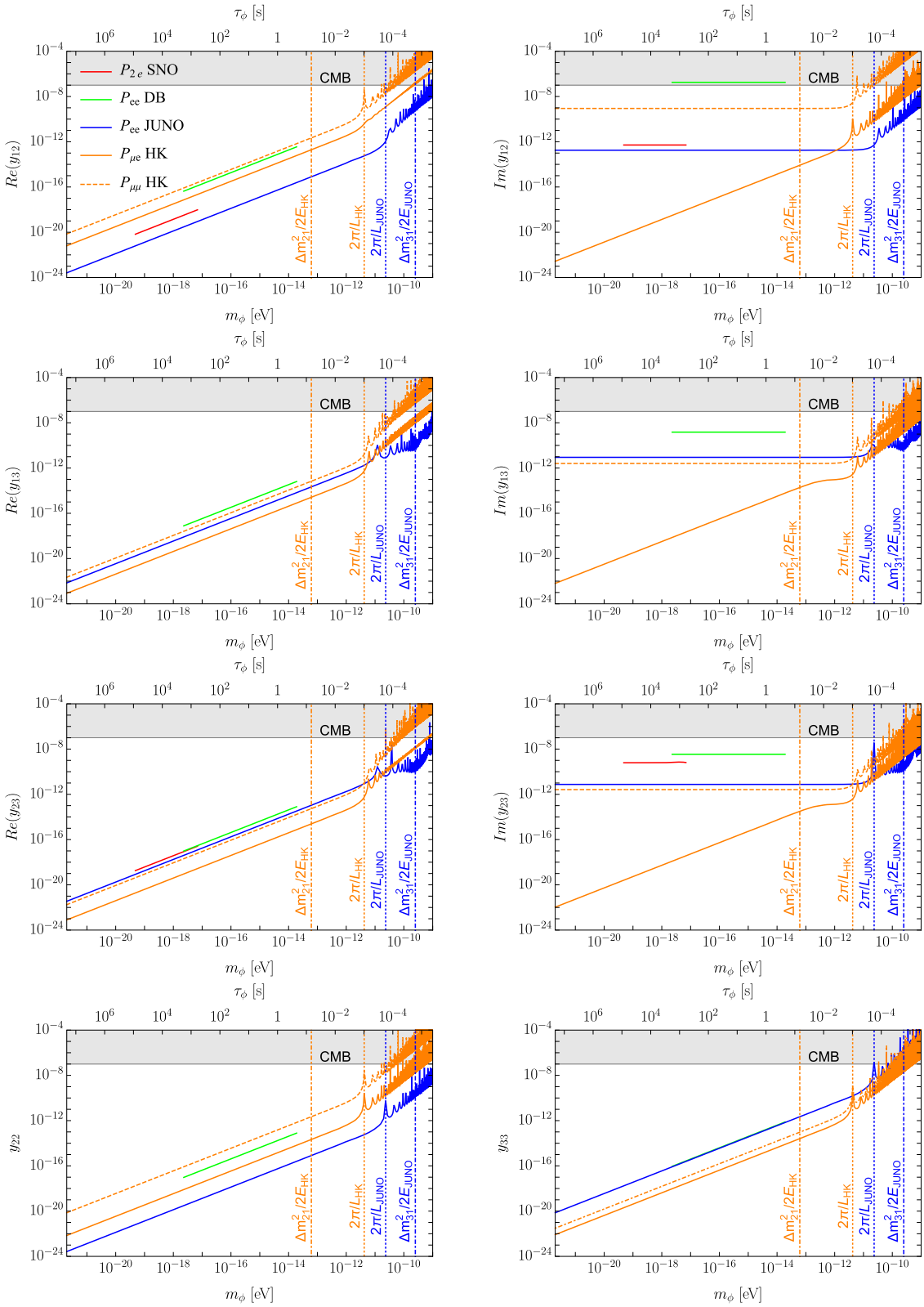

FIG. 1. Current bounds on the ULDM parameter space from Daya-Bay (DB) and SNO experiments, the projected sensitivities of JUNO and Hyper-K (HK), and the CMB bound resulting from neutrino self-interactions [21]. We assume normal hierarchy, $m_1 = 0$, $\delta_{CP} = 0$, and that the ULDM modulation amplitude is predominantly affected by a single entry of $\hat{y}$ at a time. Only statistical uncertainties are considered, based on the event collecting rate and the running time of each experiment.

matter effects, the solar neutrino flux should be constant along the year.

To calculate the first-order correction coming from the ULDM, we assume that $m_\phi \tau_\odot \ll 1$, where $\tau_\odot$ is the longest timescale for neutrino effects in the sun, such that the neutrino leaves the sun as an eigenstate of the instantaneous Hamiltonian, $\mathcal{H}(t_i) \approx \mathcal{H}_0 + \tilde{m}\sin(m_\phi(t_i - t_0))$, denoted by $\nu_m(t_i)$. We then turn to our previously obtained expressions for $P_{\alpha\beta}$, noting that $\nu_\alpha = \nu_m(t_i)$ with $m = 2$. Namely, the PMNS-like matrix $U_{\alpha i}$ should be replaced by the projection of the instantaneous mass eigenstate at time t_i onto the ULDM-independent mass eigenstates—$U_{\alpha i} \to T_{2i}(t_i)$ where $T(t_i)$ is the diagonalizing matrix of $\mathcal{H}(t_i)$ in the ULDM-independent mass basis. The deviation of $T(t_i)$ from the identity yields a first-order correction in the ULDM coupling to $\mathcal{U}^{(0)}$. When calculating $\mathcal{U}^{(1)}$, one may set $U_{\alpha i} = \delta_{2i}$, since it is already linear in the ULDM potential. For off-diagonal ULDM couplings $\hat{y}_{i2}$ with $i \neq 2$, the leading ULDM correction in our formalism is given by

$$P_{2e}^{(1)} = 2\frac{\phi_0}{E}\mathrm{Re}(U_{e2}^* U_{ei}\tilde{m}_{i2})\left(-\frac{E\sin(m_\phi(t-L-t_0))}{\Delta m_{i2}^2}\cos\frac{\Delta m_{i2}^2 L}{2E} - \cos\frac{\Delta m_{i2}^2 L}{4E}\mathrm{Im}(\kappa_{i2}) + \sin\frac{\Delta m_{i2}^2 L}{4E}\mathrm{Re}(\kappa_{i2})\right)$$
$$- 2\frac{\phi_0}{E}\mathrm{Im}(U_{e2}^* U_{ei}\tilde{m}_{i2})\left(\frac{E\sin(m_\phi(t-L-t_0))}{\Delta m_{i2}^2}\sin\frac{\Delta m_{i2}^2 L}{2E} + \cos\frac{\Delta m_{i2}^2 L}{4E}\mathrm{Re}(\kappa_{i2}) + \sin\frac{\Delta m_{i2}^2 L}{4E}\mathrm{Im}(\kappa_{i2})\right), \quad (89)$$

whereas for the diagonal coupling $\hat{y}_{22}$ and for all $\hat{y}_{ij}$ with $j \neq 2$, there are no first-order contributions to the solar probability.

The SNO Collaboration looked for a time variation in the solar neutrino flux with periods between 10 minutes and 1 day, and found a null result with a confidence level of 90% [19]. The search was expected to be sensitive (have a 90% probability of making a CL = 0.99 discovery) to sinusoidal modulations at these frequencies with an amplitude of 0.12 or greater, compared to the time-averaged flux. We may then interpret this result as a bound on the ULDM parameters, assuming m_ϕ is equal to the modulation frequency. In the $m_\phi \ll \frac{\Delta m_{i2}^2}{2E}$ limit, which applies throughout the frequency range of the analysis of [19], the correction to the solar probability in Eq. (89) becomes

$$P_{2e}^{(1)} \approx \frac{2\phi_0}{\Delta m_{i2}^2}\mathrm{Re}(U_{e2}U_{ei}^*\tilde{m}_{i2}^*)\left(-\sin(m_\phi(t-t_0)) + \frac{2Em_\phi}{\Delta m_{i2}^2}\sin\frac{\Delta m_{i2}^2 L}{2E}\cos(m_\phi(t-L-t_0))\right)$$
$$+ 4\frac{Em_\phi\phi_0}{\Delta m_{i2}^{2\,2}}\mathrm{Im}(U_{e2}U_{ei}^*\tilde{m}_{i2}^*)\left(-\cos(m_\phi(t-t_0)) + \cos\frac{\Delta m_{i2}^2 L}{2E}\cos(m_\phi(t-L-t_0))\right). \quad (90)$$

3. Constraints from neutrino self-interactions and neutrino-DM scattering

Neutrino-scalar interactions result with neutrino self-interactions. Bounds on such interactions were discussed in detail in [26]. We include the strongest bound, relevant to our parameter space, associated with the cosmic microwave background (CMB) [21] in Fig. 1.

Moreover, for large values of $\hat{y}$, neutrino-DM and neutrino-neutrino scattering may occur. If the timescale of these scatterings is much shorter than the neutrino oscillation timescale $\Delta m^2/E$ or propagation time L, the neutrino oscillations will become incoherent. As such incoherence was not observed in neutrino oscillation experiments, we infer that such high values of $\hat{y}$ are not realized in nature. For neutrino-neutrino scattering, one can estimate the scattering rate of oscillating neutrinos with the neutrino background. The most conservative estimate of this rate, assuming an MeV oscillating neutrino scattered off a massless background neutrino with temperature of 10^{-4} eV yields

$$\Gamma = \sigma n\beta \lesssim \frac{y^4}{E_{\mathrm{oscillation}}E_{\mathrm{background}}}n \lesssim \frac{y^4}{E_{\mathrm{oscillation}}T_{\mathrm{background}}} \times T_{\mathrm{background}}^3 \lesssim y^4 10^{-14}\ \mathrm{eV}, \quad (91)$$

where $E_{\mathrm{oscillation}}$ is the energy of the probed oscillating neutrino. Therefore, this rate is much slower than all timescales in question (and in particular the propagation time). For neutrino-ULDM scattering

$$\Gamma = \sigma n\beta \lesssim \frac{y^4 n}{E_{\mathrm{oscillation}}E_{\mathrm{ULDM}}}, \quad (92)$$

and therefore, considering that neutrino experiments are typically designed with $\frac{\Delta m^2 L}{E} = \mathcal{O}(1)$,

$$\Gamma L \lesssim \frac{y^4 nL}{E_{\text{oscillation}} m_\phi} \approx \frac{y^4 \rho_{\text{DM}}}{\Delta m^2 m_\phi^2} = \frac{y^4}{\Delta m^2}\left(2\ \text{GeV}\frac{10^{-12}\ \text{eV}}{m_\phi}\right)^2 \approx \left(\frac{y}{10^{-7}}\right)^4 \left(\frac{10^{-10}\ \text{eV}}{m_\phi}\right)^2 10^{-9}. \tag{93}$$

Since the experimental sensitivities to y are at least linear with m_ϕ and the CMB bound is constant in m_ϕ, this rate will not damp neutrino oscillations in the parameter space relevant for our analysis.

B. Projected sensitivities

1. Reactor experiments

In addition to current bounds from the Daya-Bay experiment, we study the projected sensitivities of ULDM parameters from other reactor neutrino experiments. We consider JUNO that measures the survival probability of $\bar{\nu}_e$ that travel ∼53 km. The energy resolution and baseline length of JUNO enable it to be sensitive to both neutrino mass squared differences Δm^2_{21} and Δm^2_{31} and thus to determine the neutrino mass hierarchy. It has an expected flux of 83 unoscillated events per day [27], and its projected sensitivity to ULDM parameters is presented in Fig. 1.

We did not consider the KamLAND experiment in our analysis, as due to its long baseline of ∼180 km it has a relatively low flux of 1–2 events per day. As opposed to accelerator experiments which fire a narrow beam of neutrinos, reactor experiments fire neutrinos uniformly in every direction, and therefore their flux decays with L^{-2}. It also collects events from different reactors with different distances, which considerably complicates the analysis.

2. Accelerator experiments

Accelerator neutrino experiments fire a beam of protons toward a target that produces charged pions. These can be manipulated into a narrow beam and decay mostly into ν_μ or $\bar{\nu}_\mu$, depending if the positive or negative pions are focused. These experiments therefore measure $P_{\mu\mu}$ and $P_{\mu e}$ (or $P_{\bar{\mu}\bar{\mu}}$ and $P_{\bar{\mu}\bar{e}}$) simultaneously. We studied the DUNE (far detector), ESS (far and near detectors), and Hyper-K experiments, out of which the latter has produced overall slightly better sensitivities to the ULDM parameters, and only these results are presented in Fig. 1. Hyper-K is expected to collect approximately 2000 to 4000 signal events in each mode of neutrinos that travel 295 km, over a run of 10 years [28].

C. Asymptotic behavior

To qualitatively understand the various plots in Fig. 1, let us consider the asymptotic behavior following from the analytical expressions we found in Sec. III. Note that we only account for the first-order corrections to the neutrino oscillation probability. Therefore, near the resonance $m_\phi = \Delta m^2/2E$ [13] the result may be inaccurate, as higher order terms would yield considerable contributions.

Let us first discuss the behavior of the CPC ULDM effects (corresponding to the plots presenting the real parts of the couplings, assuming $\delta_{\text{CP}} = 0$). For couplings that are diagonal in the unperturbed mass basis, the correction to the transition or survival probability in Eq. (45) is proportional to

$$\Sigma P^{(1)} \propto \sin\left(\frac{m_\phi L}{2}\right)\frac{2y_{ii}\phi_0}{Em_\phi} \propto \begin{cases} \frac{\text{Re}(y_{ii})}{m_\phi} & m_\phi L \ll 1, \\ \sin\left(\frac{m_\phi L}{2}\right)\frac{\text{Re}(y_{ii})}{m_\phi^2} & m_\phi L \gg 1. \end{cases} \tag{94}$$

Therefore, in an experiment sensitive to a certain value of $P^{(1)}$, the corresponding diagonal coupling y_{ii} that the experiment will be sensitive to is proportional to

$$\text{Re}(y_{ii}) \propto \begin{cases} m_\phi & m_\phi L \ll 1, \\ m_\phi^2/\sin(m_\phi L/2) & m_\phi L \gg 1. \end{cases} \tag{95}$$

We can see the transition between the two limits in the two bottom plots of Fig. 1.

As expected, when the couplings are off-diagonal, the probability also depends on the neutrino oscillation frequency, and we obtain the following relation:

$$\text{Re}(y_{ij}) \propto \begin{cases} m_\phi & L^{-1} \gg m_\phi, \\ m_\phi/\sqrt{A^2\cos^2(m_\phi L/2) + B^2\sin^2(m_\phi L/2)} & L^{-1} \ll m_\phi \ll \Delta m^2_{ij}/2E, \\ m_\phi^2/\sqrt{A^2\cos^2(m_\phi L/2) + B^2\sin^2(m_\phi L/2)} & L^{-1}, \Delta m^2_{ij}/2E \ll m_\phi, \end{cases} \tag{96}$$

where A and B are determined by the coefficients of $\text{Re}(\kappa)$ and $\text{Im}(\kappa)$ in $P^{(1)}$ according to Eq. (26), which depend on PMNS elements. If A and B are of similar magnitude, as is the case when $\text{Re}(\kappa)$ and $\text{Im}(\kappa)$ yield similar contributions to the probability, we expect the oscillations in m_ϕ to be suppressed. However, if one is much larger than the other, there are approximate poles of "bad sensitivity" around the nodes of the bigger term, at which the bound follows the

inverse of the smaller term (for example, if $A^2/B^2 \gg 1$, then around $m_\phi L/2 = n\pi$ the bound is proportional to $1/A$, while around $m_\phi L/2 = \pi/2 + n\pi$ the bound is proportional to $1/B$). This is the case when either $\mathrm{Re}(\kappa)$ or $\mathrm{Im}(\kappa)$ dominates the probability. In the case of diagonal entries of $\hat{y}$, only $\mathrm{Re}(\kappa)$ affects the probability, and therefore the bound oscillates rapidly for larger m_ϕ. For off-diagonal y entries, the modification to the CPC survival probability is affected only by $\mathrm{Re}(\kappa)$, while the transition probability is affected also by $\mathrm{Im}(\kappa)$. Therefore, the sensitivity for off-diagonal CPC couplings from measurements of survival probabilities will oscillate rapidly for larger m_ϕ, while these oscillations are suppressed for transition probabilities.

The two extreme limits of Eq. (96) are similar to the diagonal couplings case, while we may also obtain an in-between behavior if $\Delta m^2_{ij} L/(2E) > 1$. This region may be probed due to the neutrino mass hierarchy $\Delta m^2_{21} \ll \Delta m^2_{31}$, Δm^2_{32}. The JUNO experiment is designed in a way such that $\Delta m^2_{21} L/(2E) = \mathcal{O}(1)$, and $\Delta m^2_{31} L/(2E) \gg 1$. This allows for the in-between region where $L^{-1} \ll m_\phi \ll \Delta m^2_{31}/(4E)$. We can indeed see this region in the plots of y_{13}, y_{23}, but not for y_{12}.

The behavior of the CPV couplings is similar to that of the CPC couplings, with one exception: the 2-ν CPV effect. The 2-ν CPV is the only CPV effect in survival probabilities, and its mass dependence follows that of $\mathrm{Im}(\kappa_{ij})$ in Eq. (29), and thus the m_ϕ dependence of the bounds from survival probabilities is as follows:

$$\mathrm{Im}(y_{ij}) \propto \begin{cases} \mathrm{const}(m_\phi) & L^{-1} \gg m_\phi, \\ m_\phi/\sqrt{A^2\cos^2(m_\phi L/2) + B^2\sin^2(m_\phi L/2)} & L^{-1} \ll m_\phi \ll \Delta m^2_{ij}/2E, \\ m^2_\phi/\sqrt{A^2\cos^2(m_\phi L/2) + B^2\sin^2(m_\phi L/2)} & L^{-1}, \Delta m^2_{ij}/2E \ll m_\phi. \end{cases} \tag{97}$$

The main difference from the CPC bounds is in the low mass region, where the bound flattens. This is a result of the fact that in the two-generations case, as we discussed in Sec II, the only observable CPV effect comes from the time derivative of the ULDM-induced phase. The 2-ν CPV effect occurs also in transition probabilities, but overcomes the 3-ν CPV effect in the low mass region if $\Delta m^2_{21}/E \ll m_\phi \ll \Delta m^2_{31}/E$, $\Delta m^2_{32}/E$ (this effectively sets $\Delta m^2_{21} = 0$ which gives the two-neutrino picture). We can see this in-between behavior of the transition probability in Hyper-K for y_{13} and y_{23}, but not for y_{12}. Since the 2-ν CPV effect takes over at larger masses (for all off-diagonal couplings), the CPV transition probabilities would inherit the behavior of the CPV survival probabilities, which are solely affected by $\Im(\kappa)$, and thus they would significantly oscillate as a function of m_ϕ.

VI. CONCLUSIONS

The inclusion of a scalar ULDM field that couples to neutrinos provides new rich phenomenology. In this work, we have presented a generic analysis of the impact of time varying ULDM interactions with neutrinos. For the case when the ULDM rapidly oscillates during neutrino propagation, we have determined the corrections to the survival and transition probabilities for both CPC and CPV quantities. Some of the novel effects that appear are the following:

(i) A new CPV effect is present even in the two-neutrino-like case. We have also explicitly checked that in the three generation case this new effect is also present. Moreover, for three generations of neutrinos, the CPV effect does not disappear in the limit of one of the $\Delta m^2_{ij} \to 0$, and both survival and transition probabilities are modified by the new CPV effect.

(ii) The phenomena we are interested in presents oscillatory behavior, and thus we can look at the spectral power of the neutrino probabilities for angular frequencies defined by m_ϕ to determine the parameters in the model.

Interestingly, we have identified that several neutrino oscillation experiments can be sensitive to the fast variations of the ULDM field. Given this we have determined the bounds on CPC and CPV couplings from the neutrino survival probability measurements at Daya Bay and SNO. Furthermore, we have determined the sensitivity to measure the couplings at future reactor (JUNO) and long baseline neutrino oscillation experiments (DUNE, ESS, and Hyper-K).

ACKNOWLEDGMENTS

Y. N. is the Amos de-Shalit chair of theoretical physics and is supported by grants from the Israel Science Foundation (Grant No. 1124/20), the United States–Israel Binational Science Foundation (BSF), Jerusalem, Israel (Grant No. 2018257), by the Minerva Foundation (with funding from the Federal Ministry for Education and Research), and by the Yeda-Sela (YeS) Center for Basic Research. The work of G. P. is supported by grants from BSF-NSF, Friedrich Wilhelm Bessel research award, GIF, ISF, Minerva, SABRA—Yeda-Sela—WRC Program, the

Estate of Emile Mimran, and The Maurice and Vivienne Wohl Endowment. I. S. is supported by a fellowship from the Ariane de Rothschild Women Doctoral Program.

APPENDIX A: TWO GENERATIONS

For diagonal ULDM couplings, $\hat{y}_{ii}$, and $k \neq i$, the survival probability is modified by

$$P^{(1)}_{\alpha\alpha}(t) = -\sin\left(m_\phi\left(t-\frac{L}{2}-t_0\right)\right)\sin\left(\frac{m_\phi L}{2}\right)\frac{\sin^2 2\theta \hat{y}_{ii} m_i \phi_0}{E m_\phi}\sin\left(\frac{\Delta m^2_{ik} L}{2E}\right), \tag{A1}$$

where θ is the mixing angle between the unperturbed mass eigenstates and interaction eigenstates. For nondiagonal ULDM couplings $\hat{y}_{ij}$, with $i \neq j$

$$\begin{aligned} P^{(1)}_{\alpha\alpha} = \frac{\phi_0 \sin 4\theta}{E\left(\left(\frac{\Delta m^2_{ij}}{2E}\right)^2 - m^2_\phi\right)}\Bigg[&\mathrm{Im}(\hat{y}_{12})(m_1-m_2)\cos\left(m_\phi\left((t-L-t_0)+\frac{L}{2}\right)\right) \\ &\times\left(\frac{\Delta m^2_{21}}{4E}\sin\frac{\Delta m^2_{21}L}{2E}\sin\frac{m_\phi L}{2} - m_\phi \sin^2\frac{\Delta m^2_{21}L}{4E}\cos\frac{m_\phi L}{2}\right) + \mathrm{Re}(\hat{y}_{12})(m_1+m_2)\sin\left(m_\phi\left((t-L-t_0)+\frac{L}{2}\right)\right) \\ &\times\left(\frac{m_\phi}{2}\sin\frac{\Delta m^2_{21}L}{2E}\sin\frac{m_\phi L}{2} - \frac{\Delta m^2_{21}}{2E}\sin^2\frac{\Delta m^2_{21}L}{4E}\cos\frac{m_\phi L}{2}\right)\Bigg]. \end{aligned} \tag{A2}$$

APPENDIX B: MEAN VALUE OF RAYLEIGH POWER AT THE MODULATION FREQUENCY

Recall the timescales of the problem:

(1) τ_e: The running time of the experiment.
(2) $\tau_s = \frac{N_\nu}{\tau_e}$: The average spacing between events, where N_ν is the total number of measured events.
(3) τ_r: The resolution of the clock that times the events.

Therefore, during the experiment running time, there are $N_t = \frac{\tau_e}{\tau_r}$ clock ticks, each with small duration τ_r. At each clock tick we define the function:

$$h(t_i) = \begin{cases} 1 & \text{event detected,} \\ 0 & \text{no event detected.} \end{cases} \tag{B1}$$

We calculate the expectation value of the Rayleigh power spectrum, namely,

$$\begin{aligned} \langle z(f)\rangle = \frac{2}{N_\nu}\Bigg(&\left\langle\left|\sum_{i=1}^{N_t} h(t_i)\cos(2\pi t_i f)\right|^2\right\rangle \\ &+\left\langle\left|\sum_{i=1}^{N_t} h(t_i)\sin(2\pi t_i f)\right|^2\right\rangle\Bigg), \end{aligned} \tag{B2}$$

where f is the modulation frequency of the probability modulation, corresponding to $m_\phi/2\pi$. We calculate the expectation value of a generic function $F(h(t_i), t_i)$ in the sense that

$$\begin{aligned} \langle F(h(t_i), t_i)\rangle = &F(1, t_i)\cdot P(h(t_i)=1) \\ &+ F(0, t_i)\cdot P(h(t_i)=0), \end{aligned} \tag{B3}$$

where the probability that an event is detected is given by

$$\begin{aligned} P(h(t_i)=1) &= \frac{N_\nu}{N_t}[1+\epsilon\sin(2\pi t_i f)] \\ &= N_\nu\frac{\tau_r}{\tau_e}[1+\epsilon\sin(2\pi t_i f)], \end{aligned} \tag{B4}$$

where ϵ is the amplitude of the modulation. We assumed for simplicity that the phase of the modulation is zero, such that it appears as a sine, but the final result holds for a generic phase. Let us start with calculating the expectation value of the sine term. Notice that

$$\begin{aligned} \left\langle\left|\sum_{i=1}^{N_t} h(t_i)\sin(2\pi t_i f)\right|^2\right\rangle = &\mathrm{Var}\left(\sum_{i=1}^{N_t} h(t_i)\sin(2\pi t_i f)\right) \\ &+\left\langle\left|\sum_{i=1}^{N_t} h(t_i)\sin(2\pi t_i f)\right|\right\rangle^2. \end{aligned} \tag{B5}$$

Calculating the variance term first,

$$\begin{aligned}\mathrm{Var}[h(t_i)\sin(2\pi t_i f)] &= \langle h^2(t_i)\sin^2(2\pi t_i f)\rangle \\ &\quad - \langle h(t_i)\sin(2\pi t_i f)\rangle^2 \\ &= (P(t_i) - P^2(t_i))\sin^2(2\pi t_i f) \\ &\approx \frac{N_\nu}{N_t}[1+\epsilon\sin(2\pi t_i f)]\sin^2(2\pi t_i f)).\end{aligned} \tag{B6}$$

In the last approximation we assume $\frac{N_\nu}{N_t} \ll 1$, which is equivalent to the statement that the resolution of the clock is much better than the typical time between events. The variance of sum is simply the sum of variances, since in our case the measurements at different times are uncorrelated; thus,

$$\begin{aligned}&\mathrm{Var}\left(\sum_{i=1}^{N_t} h(t_i)\sin(2\pi t_i f)\right) \\ &= \sum_{i=1}^{N_t}\frac{N_\nu}{N}[1+\epsilon\sin(2\pi t_i f)]\sin^2(2\pi t_i f).\end{aligned} \tag{B7}$$

Changing variables,

$$t_n \to n\tau_{\mathrm{res}}, \tag{B8}$$

$$0 < n \le N_t, \tag{B9}$$

we obtain

$$\begin{aligned}\mathrm{Var}\left(\sum_{i=1}^{N_t} h(t_i)\sin(2\pi t_i f)\right) &= \frac{N_\nu}{N_t}\left[\sum_{n=1}^{N_t}\sin^2(2\pi n\tau_{\mathrm{res}} f)\right. \\ &\quad \left. + \epsilon\sum_{n=1}^{N_t}\sin^3(2\pi n\tau_{\mathrm{res}} f)\right].\end{aligned} \tag{B10}$$

The first term yields

$$\begin{aligned}\sum_{n=1}^{N_t}\sin^2(2\pi n\tau_{\mathrm{res}} f) &\approx \int_0^{N_t} dz\sin^2(2\pi z\tau_{\mathrm{res}} f) \\ &= \frac{N_t}{2}[1-\mathrm{sinc}(4\pi N_t\tau_{\mathrm{res}} f)] \\ &\approx \frac{N_t}{2},\end{aligned} \tag{B11}$$

where we use the approximation

$$N_t\tau_{\mathrm{res}} f = \tau_{\mathrm{exp}} f \gg 1. \tag{B12}$$

The second term gives

$$\sum_{n=1}^{N_t}\sin^3(2\pi n\tau_{\mathrm{res}} f) \approx \int_0^{N_t} dz\sin^3(2\pi z\tau_{\mathrm{res}} f) = \frac{2N_t(2+\cos(2fN_t\pi\tau_{\mathrm{res}}))\sin^3(fN_t\pi\tau_{\mathrm{res}})}{3}\mathrm{sinc}(fN_t\pi\tau_{\mathrm{res}}), \tag{B13}$$

and may therefore be neglected under the approximation in Eq. (B12). The second term in Eq. (B15) is

$$\left\langle\left|\sum_{i=1}^{N_t} h(t_i)\sin(2\pi t_i f)\right|\right\rangle^2 = \left|\sum_{i=1}^{N_t} P(t_i)\sin(2\pi t_i f)\right|^2 = \left[\sum_{i=1}^{N_t}\frac{N_\nu}{N_t}[1+\epsilon\sin(2\pi t_i f)]\sin(2\pi t_i f)\right]^2 = \frac{\epsilon^2}{4}N_\nu^2. \tag{B14}$$

Finally, we get

$$\left\langle\left|\sum_{i=1}^{N_t} h(t_i)\sin(2\pi t_i f)\right|^2\right\rangle = \frac{N_\nu}{2} + \frac{\epsilon^2}{4}N_\nu^2, \tag{B15}$$

$$\left\langle\left|\sum_{i=1}^{N_t} h(t_i)\cos(2\pi t_i f)\right|^2\right\rangle = \frac{N_\nu}{2}, \tag{B16}$$

and thus

$$\langle z(f)\rangle = 2 + \frac{\epsilon^2}{2}N_\nu. \tag{B17}$$

[1] Gordan Krnjaic, Pedro A. N. Machado, and Lina Necib, Distorted neutrino oscillations from time varying cosmic fields, Phys. Rev. D **97**, 075017 (2018).
[2] Vedran Brdar, Joachim Kopp, Jia Liu, Pascal Prass, and Xiao-Ping Wang, Fuzzy dark matter and nonstandard neutrino interactions, Phys. Rev. D **97**, 043001 (2018).
[3] Francesco Capozzi, Ian M. Shoemaker, and Luca Vecchi, Neutrino oscillations in dark backgrounds, J. Cosmol. Astropart. Phys. 07 (2018) 004.
[4] Asher Berlin, Neutrino Oscillations as a Probe of Light Scalar Dark Matter, Phys. Rev. Lett. **117**, 231801 (2016).
[5] Abhish Dev, Pedro A. N. Machado, and Pablo Martínez-Miravé, Signatures of ultralight dark matter in neutrino oscillation experiments, J. High Energy Phys. 01 (2021) 094.
[6] Marta Losada, Yosef Nir, Gilad Perez, and Yogev Shpilman, Probing scalar dark matter oscillations with neutrino oscillations, J. High Energy Phys. 04 (2022) 030.
[7] Eung Jin Chun, Neutrino transition in dark matter, arXiv:2112.05057.
[8] Guo-yuan Huang and Newton Nath, Neutrino meets ultralight dark matter: $0\nu\beta\beta$ decay and cosmology, J. Cosmol. Astropart. Phys. 05 (2022) 034.
[9] Gonzalo Alonso-Álvarez, Katarina Bleau, and James M. Cline, Distortion of neutrino oscillations by dark photon dark matter, Phys. Rev. D **107**, 055045 (2023).
[10] Abhish Dev, Gordan Krnjaic, Pedro Machado, and Harikrishnan Ramani, Constraining feeble neutrino interactions with ultralight dark matter, Phys. Rev. D **107**, 035006 (2023).
[11] Dawid Brzeminski, Saurav Das, Anson Hook, and Clayton Ristow, Constraining vector dark matter with neutrino experiments, arXiv:2212.05073.
[12] Guo-yuan Huang, Manfred Lindner, Pablo Martínez-Miravé, and Manibrata Sen, Cosmology-friendly time-varying neutrino masses via the sterile neutrino portal, Phys. Rev. D **106**, 033004 (2022).
[13] Marta Losada, Yosef Nir, Gilad Perez, Inbar Savoray, and Yogev Shpilman, Parametric resonance in neutrino oscillations induced by ultra-light dark matter and implications for KamLAND and JUNO, J. High Energy Phys. 03 (2023) 032.
[14] S. M. Bilenky, J. Hošek, and S. T. Petcov, On the oscillations of neutrinos with dirac and Majorana masses, Phys. Lett. B **94**, 495 (1980).
[15] Carlo Giunti, No effect of Majorana phases in neutrino oscillations, Phys. Lett. B **686**, 41 (2010).
[16] A. Yu. Smirnov, The geometrical phase in neutrino spin precession and the solar neutrino problem, Phys. Lett. B **260**, 161 (1991).
[17] Evgeny K. Akhmedov, A. Yu. Smirnov, and P. I. Krastev, Resonant neutrino spin flip transitions in twisting magnetic fields, Z. Phys. C **52**, 701 (1991).
[18] L. Wolfenstein, Neutrino oscillations in matter, Phys. Rev. D **17**, 2369 (1978).
[19] B. Aharmim *et al.*, Searches for high frequency variations in the ^{8}B solar neutrino flux at the sudbury neutrino observatory, Astrophys. J. **710**, 540 (2010).
[20] Eilam Gross and Ofer Vitells, Trial factors for the look elsewhere effect in high energy physics, Eur. Phys. J. C **70**, 525 (2010).
[21] Francesco Forastieri, Massimiliano Lattanzi, and Paolo Natoli, Cosmological constraints on neutrino self-interactions with a light mediator, Phys. Rev. D **100**, 103526 (2019).
[22] D. Adey *et al.*, Search for a time-varying electron antineutrino signal at Daya Bay, Phys. Rev. D **98**, 092013 (2018).
[23] Feng Peng An *et al.*, Measurement of electron antineutrino oscillation based on 1230 days of operation of the Daya Bay experiment, Phys. Rev. D **95**, 072006 (2017).
[24] J. Yoo *et al.*, A search for periodic modulations of the solar neutrino flux in Super-Kamiokande I, Phys. Rev. D **68**, 092002 (2003).
[25] N. Tolich, Sudbury neutrino observatory: Latest results and future prospects, Nucl. Phys. B, Proc. Suppl. **217**, 107 (2011).
[26] Jeffrey M. Berryman *et al.*, Neutrino self-interactions: A white paper, Phys. Dark Universe **42**, 101267 (2023).
[27] Agnese Giaz, Status and perspectives of the JUNO experiment, in *Prospects in Neutrino Physics* (London, UK, 2018), pp. 53–60.
[28] E. Kearns *et al.*, Hyper-Kamiokande physics opportunities, in *Community Summer Study 2013: Snowmass on the Mississippi* (Minneapolis, MN, 2013), arXiv:1309.0184.